SME Annual Meeting
Feb. 21 - 24, 2016, Phoenix, AZ

Preprint 16-100

CURRENT ISSUES WITH PURPORTED "ASBESTOS" CONTENT OF TALC: PART 2, EXAMPLES IN HYDROTHERMAL HOSTED TALC ORES

M. Buzon, Univ. of Idaho, Moscow, Idaho
M. Gunter, Univ. of Idaho, Moscow, Idaho

ABSTRACT

Talc formed by hydrothermal alteration of preexisting carbonate rocks is known to be nearly monomineralic, and lacking in amphiboles. In southwest Montana, talc formed from hydrothermally altered dolomitic marbles, and is still actively mined. These talc deposits are typically in contact with quartzofeldspathic gneiss and marble. Accessory minerals vary between these rocks and the ore producing body; the identification and characterization of such minerals requires carefully selected analytical methods. Recent litigation and ensuing confusion over the petrology and asbestos content of these deposits challenges the talc mining industry in Montana, and elsewhere in the world.

INTRODUCTION

Commercial talc has been mined from the deposits in southwest Montana since the 1940s, and by 1956 the region had output 200,000 tons of talc ore (Chidester et al., 1964). Commercial talc refers to rocks containing more than 20% of the mineral talc (McCarthy et al., 2006); the ores from Montana typically contain upwards of 90% talc. This region remains the leading domestic source of talc in the U.S. partly due to the reserves in the area, and partly due to the diagnostic purity of the ore compared to that of other regions, some of which are no longer actively mined. The mineral talc, a sheet silicate, is expressed by the formula $Mg_3Si_4O_{10}(OH)_2$, and therefore can form in geologic environments that are rich in Mg, Si, O and water. The protolith for the talc deposits in southwest Montana is a dolomitic marble, but other common protoliths include ultramafic igneous, mafic igneous, and siliceous dolomites (McCarthy et al., 2006). Physical properties such as hardness of 1 on Mohs hardness scale, white streak and slippery feel are among some of the reasons why talc is so widely used as fillers in a number of industries. In decreasing order, ceramics, paper, paint, roofing, plastics, rubber, and cosmetics are the leading domestic industries that use talc despite the decreasing trend in U.S. talc use and production since 1994 (Virta, 2015). The purpose of this paper is to describe the mechanism of talc formation in southwest Montana by focusing on talc deposits and surrounding rocks in the Ruby, Greenhorn, and the Gravelly Ranges, and to relate the mechanism of formation to the composition of talc ores. The compositional data show mineral content of selected ores, and the major and trace element content of those minerals, specifically talc. Our electron microprobe (EPMA), powder x-ray diffraction (XRD) and x-ray fluorescence data for samples from five mines in these three ranges provide continued evidence of the purity of these ores despite claims made during recent litigation that these ores contain asbestos. The five mines that we discuss include the Beaverhead, Treasure, Regal, Willow Creek, and Yellowstone Mines (Figure 1.)

HYDROTHERMALLY ALTERED CARBONATE TALC DEPOSITS

Most economic talc deposits are formed from altered carbonate rocks, as opposed to rocks of ultramafic or mafic origin; those that have been metasomatically altered produce the most pure talc ores (Van Gosen et al., 2004). Metasomatism is the solid-state interaction between rock and aqueous fluids, which introduce or remove chemical components. This process differs from isochemical metamorphism in that ions or ionic groups are perfectly mobile in solution, instead of H_2O or CO_2 being the only mobile components. This type of reaction generally produces rocks that have fewer phases than those created by replacement metamorphism, and results in a rock with a different composition than the protolith. The number of phases tends to increase in the altered rock with distance from the fluid source, as alteration is less extensive. These rocks, assuming no late-stage regional metamorphism follows, are likely to be granoblastic (polygonal grain boundaries, random orientation of grains, equigranular) and lack foliation (Zharikov et al., 2007). Pseudomorphs after protolith minerals in metasomatic rocks are common, as can be seen in Figure 2, which shows talc that has crystallized after a carbonate mineral.

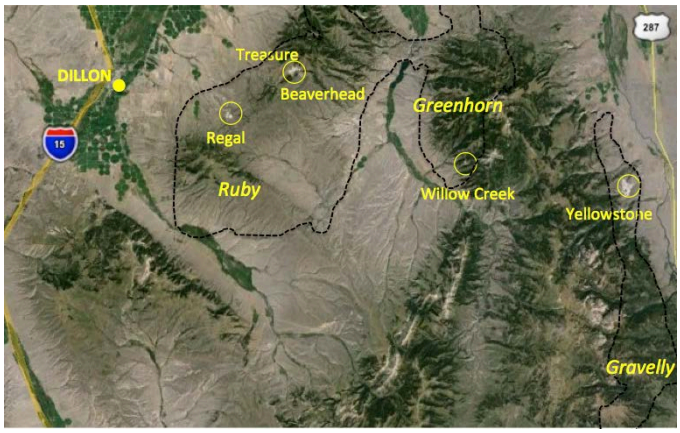

Figure 1. The five mine locations are labeled on the Google Earth image of Madison County, Montana. The width of the image is approximately 57 miles. Dashed lines based on Dahl (1979) indicate Precambrian rocks. The Beaverhead, Treasure and Regal Mines are in the Ruby Range. The Beaverhead and Treasure Mines are adjacent, and are located in the same circle in this diagram. Beaverhead is to the southeast of Treasure. The Willow Creek and Yellowstone Mines are located in the Greenhorn and Gravelly Ranges, respectively.

In the case of hydrothermally altered talc deposits, aqueous fluids transport silica, which interacts with dolomitic marbles. The silica is sourced from a nearby SiO_2-rich lithology, and the fluids are typically introduced to the system through pre-existing faults or fractures. Regardless of the source of the fluids, which may include but is not limited to meteoric waters, connate brines, seawater, or a combination of sources, these deposits form in environments where there were high volumetric fluid/rock ratios, on the order of several hundred to 1000 (Moine et al., 1989, Anderson et al., 1990). Heat from igneous activity and hydrostatic pressure are the driving forces behind circulating the talc-forming fluids. This general process has occurred in the Allamoore mining district in west Texas, Talc City west of Death Valley in California, Southwest Montana, as well as in a number of other locations worldwide (Van Gosen et al., 2004, Tornos and Spiro, 2000, Moine et al. 1989). Another common trait among these deposits is that they have polymetamorphic histories, at least requiring for dolomitization to have occurred before talc crystallization.

SOUTHWEST MONTANA TALC FORMATION

The talc deposits in southwest Montana have a long metamorphic history involving at least three events that will be referred to as M_1, M_2, and M_3. The talc formed in dolomitized marbles of the Cherry Creek

rocks, which can be most simply described as Archean meta-sediments. Other Cherry Creek rock types include metamorphosed carbonates, mafic gneiss, banded iron formation, meta-pelites and quartzites (Berg 1979, Dahl 1979). This group of rocks exists in multiple ranges through southwest Montana but is not easily traceable due to prominent foliation and isoclinal folds. The Dillon Gneiss has a quartzofeldspathic composition and conformably underlies the Cherry Creek dolomites. This gneiss was most likely a source of SiO_2 in the formation of talc. Despite the structural complexity of the area, it is generally assumed that the talc in southwest Montana all has similar, if not the same geologic history because it only occurs in Precambrian rocks, and is not found in Paleozoic dolomites. The ternary diagrams in Figures 3A-3B from Anderson et al. (1990) plot the bulk compositions determined from XRF analyses of high-grade marbles (rock compositions formed from M_1), talc-bearing marbles (rock compositions formed from M_2), and massive talc bodies (rock compositions formed from M_3). These diagrams are helpful in describing the compositional variations that accompanied geologic events in the Ruby Range. H_2O and CO_2 are not included in these diagrams because they are mobile components and are assumed to be very abundant. Again, due to the structural and lithological constraints on talc occurrences in southwest Montana, the deposits in the Ruby Range, Greenhorn Range and Gravelly Range are understood to have very similar histories.

Figure 2. The rhombohedral cleavage is still dominant in this talc sample collected in the Treasure Mine (Ruby Range). The scale on the pencil is in cm.

M_1

Approximately 2.7Ga upper-amphibolite facies metamorphism (M_1) of the Cherry Creek rocks occurred (James and Hedge 1980) which resulted in the formation of high-grade marbles. Peak metamorphic conditions from this event based on mineral-pair geothermometers and geobarometers recorded in two areas in the Ruby Range span from 675 ± 45° - 745 ± 50°C and 0.5-0.8 GPa respectively (Dahl, 1979). This event also created the dominant northeast-trending, northwest dipping foliation and axial surfaces in isoclinal folds (Anderson et al., 1990**)**. The M_1 mineral assemblage in the marble included calcite – olivine – phlogopite ± dolomite ± garnet, with tremolite replacing olivine. The formation of tremolite is not completely understood but it is likely that it formed as a late M_1 mineral or an early M_2 mineral. (Anderson et al.) The compositions for these rocks are plotted as squares in Figure 3A.

M_2

Retrograde greenschist metamorphism (M_2) occurred during the Meso-Paleoproterozoic and resulted in the formation of talc-bearing marbles from the alteration of high-grade marbles. Biotite and muscovite in the Dillon gneiss reveal K-Ar dates of 1.6±0.1Ga (Giletti, 1966**)** (M_2). Similar $^{39}Ar/^{40}Ar$ dates in phlogopite from marbles and amphibolites were recorded for ~1.7Ga (Brady et al., 1998). This event overprinted the earlier high-grade metamorphism and is associated with the increase in Mg in the region, recorded by dolomitization of the high-grade marbles and clinochlore (chlorite Mg end-member) replacement of plagioclase and biotite in the Dillon Gneiss. This is shown by trend 1 in Figure 3B. Chloritization of the gneiss occurred where it is adjacent to the marbles or talc bodies, suggesting that the current compositions of the rocks resulted from the same process (Anderson et al., 1990). Another important point is that dolomitization of calcite would have resulted in a volumetric decrease due to the replacement of Ca^{2+} by Mg^{2+}. There is no evidence for volume loss indicating that Mg was present in excess. The question remains for what such a massive source for Mg would have been. Events M_2 and M_3 are gradational rather than recorded by specific dates. The inclusions of chlorite in the massive talc bodies indicate the two crystallized during the same or overlapping processes, but we know that the introduction of Mg to the system happened prior to the formation of the very pure talc. The bulk XRF data from Anderson et al (1990) plot the talc-bearing marbles at a composition very close to pure dolomite. These rocks have not been completely altered to talc due to the lack of SiO_2. The mineral assemblage associated with these conditions is talc – dolomite – chlorite ± calcite. Accessory minerals include graphite, pyrite, manganese oxides and quartz (Anderson et al., 1990). These rocks are not ore-quality.

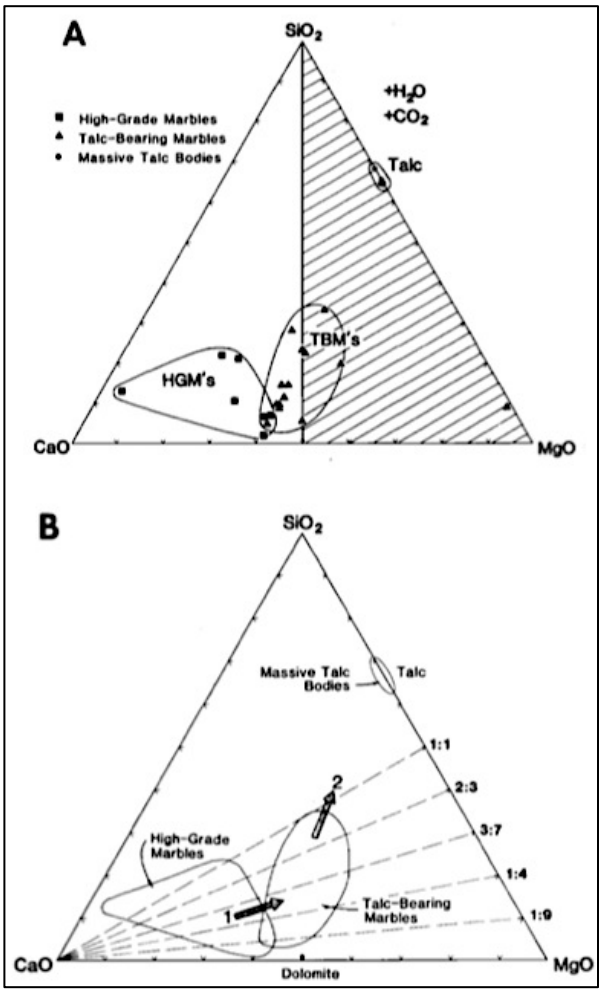

Figures 3A-3B. (Figure 11 from Anderson et al. 1990) A: High-grade marbles (HGM), talc-bearing marbles (TBM) and massive talc bodies (talc) plotted in the CaO-MgO-SiO_2 ternary diagram based on bulk XRF analyses (Table 2 in Anderson et al., 1990). There is little overlap between fields. B: Arrow 1 follows the compositional trend from HGM to TBM, increase in MgO/CaO. Arrow 2 follows compositional trend from TBM-talc, increase in SiO_2/MgO.

M_3

The metasomatic event (M_3) is estimated to have occurred 1.6-1.1Ga. A series of mafic dikes and sills intruded the Archean rocks approximately 1.455Ga and 1.12-1.13 Ga, accompanied by extension associated with rifting of the overlying basin. These dikes are thought to be the heat source behind circulating the talc forming fluids. Anderson et al. (1990) estimated the conditions for the talc-forming event from samples in the Ruby Range to be <400°C and 2Gpa, indicating a depth of about 6km. Volumetric water/rock ratios were calculated to be >600. Brady et al. (1998) determined stable C isotope ratios in carbonates and graphite in high-grade marbles and talc rocks from the Ruby Range. Their study determined that the ^{14}C values were indistinguishable and represented amphibolite-grade conditions (M_1). The talc-forming fluids did not affect the ^{14}C composition, indicating that the fluid was CO_2-poor. Differences in the ^{18}O in dolomite and calcite indicate the fluids were H_2O-rich and thought to be derived from seawater. In the same study the temperatures of talc formation were constrained to 200°-300°C, at depths of 5-10 km. Their study also determined $^{40}Ar/^{39}Ar$ ages for muscovite intergrown with talc at 1.36Ga. This date coincides with the timing of the mafic intrusions. Gammons and Matt (2002) studied fluid inclusions in quartz samples that were contemporaneous with talc from the Gravelly Range. Their results indicate the talc-forming fluids were 7x saltier than modern day seawater and that trapping temperatures were 190°-250°C. Their suggested mechanism is that connate brines and Proterozoic seawater associated with the overlying Belt Basin were heated by mafic intrusions and were circulated toward the underlying Cherry Creek rocks. Circulation may have been aided by the high-pressure gradient due to the thick overlying Belt sequence and from the volume increase resulting from heating the brines. Estimated depths are from 3-10km. Figure 4, is a schematic of this process. Botryoidal talc has been found at the Yellowstone and other mines, which indicates crystallization in a shallow vug-like environment (Cerino et al., 2007, Underwood et al., 2014). It is possible that talc with this texture was formed in the waning stages of M_3 as a result of lower pressures, however significant decreases in pressure would have had to occur for small cavities to exist. This texture is not observed homogeneously throughout the deposits and may have been controlled by small-scale structural differences.

Despite differences in P-T estimates for formation of the massive talc bodies, it is agreed upon that the following reaction:

$$3 \text{ dolomite} + 4 SiO_2(aq) + 4H_2O = 1 \text{ talc} + 3Ca^{2+} + 6HCO_3^-,$$

occurred, and that temperatures <400°C resulted in the pure talc mineralogy. Generally, the massive talc bodies lack carbonates and other Ca-rich phases, indicating that the fluid was not rich in CO_2 or Ca^{2+}. The $SiO_2(aq)$ was sourced from the quartzofeldspathic gneiss reacting with the seawater-brine fluid. Arrow 2 in Figure 3B illustrates the increasing amount of SiO_2 in the system. Trends 1 and 2 have different slopes, supporting the idea that the increase in MgO and increase in SiO_2 were two separate processes (Anderson et al., 1990).

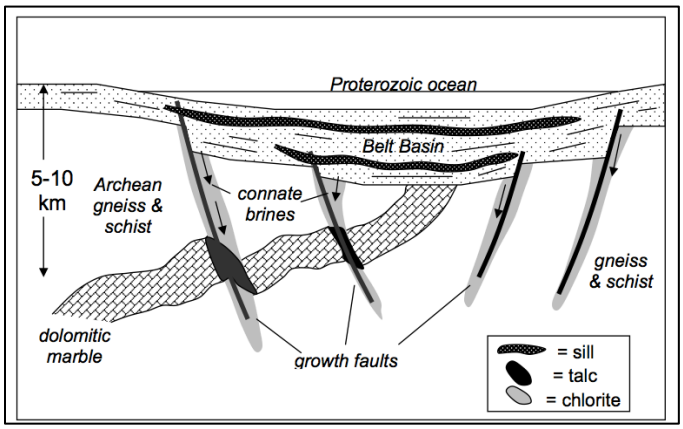

Figure 4. (Gammons and Matt, 2002, Figure 6) Schematic of talc-forming mechanism.

One suggestion made during testimony and in a deposition by a plaintiff's expert in civil litigation has been made that the talc deposits in southwest Montana were formed by interactions with the Yellowstone hot spot. The timescale for talc formation, for which there is an abundance of thermochronometric data, occurred on the scale of 1-2 Ga, and the Yellowstone hot spot has a history <20Ma, much closer to <5Ma if there would be any effects in southwest Montana. If the hot spot had resulted in alteration of these rocks we would see evidence of hydrothermal alteration in all the rocks older than 5Ma. The talc in this region is found in Archean dolomites, and not found in younger carbonates. This suggestion has no validity in describing the mechanism of talc formation in southwest Montana. There are many occurrences of talc around the world that have formed by hydrothermal or precipitate mechanisms (Evans and Guggenheim, 1988), but these are not in deposits at a mineable scale.

WILLOW CREEK MINE

The Willow Creek mine was the largest source of commercial talc in the Greenhorn Range. There have been recent claims in civil litigation that asbestiform tremolite, chrysotile and anthophyllite have been found in this deposit and represent the mineralogy of the ores once mined here. Although this deposit is no longer a source for commercial talc, these claims have serious consequences for the entire talc-producing region. Also, Cyprus Mines Corporation found occurrences of fibrous tremolite down dip from the former pit (Weeks, 1984); however as is common, the authors of this study did not define fibrous. We would like to address the occurrences of the abovementioned minerals, and give context for the importance of where these minerals occur. But before we provide our research, it is worth pointing out that to our knowledge in the publishing literature there are no reports of asbestos minerals occurring in talc formed in southwestern Montana in general or at Willow Creek specifically. In fact both Berg (1979) and Van Gosen et al. (2004) point out the former, while Berg (1979) points out the latter as well.

Asbestos content

The purity of a talc deposit is unique to the mechanism and composition of geologic materials from which it formed. For example talc mined from metamorphosed carbonate deposits can contain significant amounts of amphiboles. Although these ores filled an economic niche for decades, some of which are tabulated in Chidester et al., (1964), it is now well understood that the use of them is no longer suitable in many industries due to potential asbestos exposure. The regulatory definition of asbestos in the Code of Federal Regulations is, "chrysotile, amosite, crocidolite, tremolite asbestos, anthophyllite asbestos, actinolite asbestos, and any of these minerals that have been chemically treated and/or altered" (29CFR§1910.1001(b)). Although the word asbestos is used in the legal definition, "tremolite asbestos" is tremolite that displays a fibrous, or hair-like habit, the same goes for the other five asbestos minerals. These minerals are not regulated when they do not occur in a fibrous habit. Asbestos is a commercial term for minerals that have a fibrous morphology, high tensile strength, flexibility and are heat resistant. These minerals are of concern in talc products because they are known to form in some economic talc deposits. Many commercial talc products are processed into very fine, potentially respirable grain sizes, so those that do contain asbestos minerals would serve as a pathway for exposure and the associated lung diseases for people who are regularly exposed to these commercial talcs.

Tremolite ($Ca_2Mg_5Si_8O_{22}(OH)_2$) and anthophyllite ($Mg_7Si_8O_{22}(OH)_2$) are the most likely of the amphibole varieties to occur in talc deposits. The deposits that do contain amphiboles in greater than trace concentrations have been formed by contact or regional metamorphism, at higher temperatures (>400°C) and/or higher pressures than what was required to form talc in a predominantly metasomatic zone (Van Gosen et al., 2004). An example of this would be the deposits in upstate/central New York that produced ores containing minor to major concentrations of tremolite and anthophyllite. These deposits formed from regional metamorphism accompanied shortly after by related hydrothermal alteration (Chidester et al., 1964**)** Fluids are involved in nearly all metamorphic reactions, but unlike the deposits in New York, the deposits in southwest Montana have undergone extensive hydrothermal alteration. The tremolite identified in the deposit at Willow Creek is located in dolomitic and calcitic marbles. These rocks do not represent

M_3 mineral assemblages associated with talc ores Of the sixteen cores that were taken during the 1979-1984 study, only one was representative of talc ore, which contained trace concentrations of tremolite. Berg's (1979) observations of tremolite were limited to the marbles, and were not associated with the massive talc-body, which generally agrees with the results of the mine report. The presence of tremolite may serve as an indicator for the edge of the metasomatic zone at Willow Creek for two reasons: 1) tremolite is not stable in the temperature ranges estimated for the M_3 event, and 2) the metasomatic fluids resulted in rocks with a much higher Si/Mg ratio, and lower Ca than what is suitable for tremolite to form.

The non-amphibole variety of asbestos, chrysotile ($Mg_3Si_2O_5(OH)_4$) is a serpentine-group mineral. There are three Mg-serpentine-group minerals, but chrysotile is the only one that is regulated. Serpentine is often seen replacing forsterite in metamorphic rocks, creating the classic mesh texture. Anderson et al. (1990) pointed this out in their petrographic descriptions of the high-grade marbles, which has an assemblage of minerals that reflect amphibolite-grade metamorphism. This reaction is not preserved in the massive talc bodies because of the high Si:Mg ratio introduced by the pervasive altering fluids, and the lower temperatures required to stabilize talc. The serpentine that has been found in association with the talc deposits in this region has not been found in the massive talc body, and therefore, regardless of morphology, has no commercial pathway that would be a concern for human exposure. We are not claiming that chrysotile, or another serpentine-group mineral does not occur anywhere in the altered Cherry Creek rocks.

Sepiolite ($Mg_8Si_{12}O_{30}(OH)_4(H_2O)_2$), is a sheet silicate that has been identified at the Willow Creek Mine, but has never warranted much attention until recently. It occurs in a fibrous habit, and some samples have a waxy, plastic-like appearance that could easily be mistaken for an asbestos variety without close observation and the application of appropriate analytical methods. For example, energy-dispersive spectroscopy (EDS), a commonly used semi-quantitative compositional technique yields, element concentrations as the area under peaks (often simplified to peak height). The ratio of Si/Mg in anthophyllite and sepiolite is 1.73, making the two difficult to confidently distinguish based on EDS because the relative Mg and Si peak heights will be the same for these two minerals. Structurally the two are distinct, but both have a 5.3 Å repeat (along the polymerized chains of silicon tetrahedral from which they form- double chains for anthophyllite and triple chains for sepiolite), so diffraction patterns on a selected area, and grain orientation can also lead to misidentifying these phases. Claims of sepiolite and chrysotile in bundles together brings up two considerations. First, because the two are both sheet silicates (like talc) they share have the structural similarity of ~5.3 Å repeat along the a-axis. This could make the two difficult to distinguish without other crystallographic identifiers.

SAMPLES AND MINES

The samples at the focus of this paper are talc-rich, commercial grade rocks. The Willow Creek Mine and Beaverhead Mine, last operated by Cyprus Industrial Minerals are no longer actively mined. The mine site at Willow Creek has been reclaimed, but reprehensive talc samples were collected in the area of the former, now collapsed pit (WC_1a and WC_8a). The sample from the Beaverhead Mine (BH) was a split that was provided by Richard Berg. The Yellowstone Mine, operated by Imerys Talc is the leading producing mine in the region. Samples from this mine include a low-grade (YE_low) and high-grade ore (YE_high). The Treasure and Regal Mines, operated by Barretts Minerals Inc., a subsidiary of Minerals Technologies Inc., are also currently operating. The samples from these two mines range in quality from float (TR_float) to high-grade ores (Tr_G1, RE).

METHODS

Eight samples will be discussed in this paper. All were prepared for electron probe micro-analysis, seven for powder x-ray diffraction, and five were prepared for x-ray fluorescence spectrometry.

Powder XRD

Approximately four grams of each talc sample were ground with a mortar and pestle until fragments were ~2mm in diameter. Samples were then ground in a polyethelene canister with corundum milling beads using a McCrone micronizing mill for 12 minutes with 95% ethanol. The slurry was rinsed into a glass dish and the powdered contents were scratched from the glass dish after the ethanol evaporated. We prepared backfilled powder mounts and analyzed samples with the Siemens D5000 powder x-ray diffractometer at the University of Idaho from 2°-52°, for 20 seconds for each step of 0.020°. The samples were hit with Cu kα radiation. Phases were identified using the EVA software and accompanying database. The same powders were used for bulk x-ray fluorescence (XRF) analyses.

Bulk XRF

The powdered samples were used to make fused glass beads for bulk XRF analyses using the ThermoARL X-ray fluorescence spectrometer at Washington State University's GeoAnalytial Laboratory. Each bead required 2.0-3.5 grams of powdered sample, along with a powdered Li-tetraborate flux; a sample-to-flux ratio of 1:2 was required. The sample and flux were weighed and combined in a plastic mixing jar, and were thoroughly mixed. The contents of the jar were poured into a graphite crucible which was put on a silica slab and placed in a furnace with an internal temperature of 1000 °C. After the crucible contents melted the slab was removed from the furnace, the samples were allowed to cool into fused glass beads and were removed from the crucibles. Samples were ground in a tungsten-carbide mill and re-fused into homogenous glass beads. The procedure we followed is detailed in Johnson et al. (1999).

EPMA

Individual mineral grains were analyzed in prepared thin sections by the JEOL JXA-8500f field emission electron microprobe at Washington State University. Thin sections were prepared by Burnham Petrographics from Rathdrum, Idaho; four ~1cm wide samples were mounted on one standard sized thin section slide. The slides were inspected using a polarized light microscope, and reference targets were marked on the thin sections with a fine-point felt pen. This is the dark rim in many of the BSE and XPL images. The electron beam was set to 20kV accelerating voltage and 30nA beam current. Samples were analyzed with a 5µm beam and standards were analyzed with a 10µm beam. BSE images were collected for all targets and are shown in Figures 6-13.

RESULTS AND DISCUSSION

Powder XRD

Figure 5A (Yellowstone and Willow Creek Mines) and 5B (Ruby Range Mines) include powder x-ray diffraction spectra for seven samples. Predominant peaks for clinochlore and talc are labeled. Only talc was detected in the high- and low-grade ores from the Yellowstone Mine. Willow Creek_1a is mostly talc but does have a detectable amount of clinochlore in it. Only talc was detected in sample 8 from Willow Creek. The three samples from the Ruby Range are predominantly talc as well, with only a trace amount of clinochlore detected in the samples from the Regal and the Beaverhead Mines. Most of these samples were obtained with the idea that they were ore quality, so these results were expected. Sample 1a from Willow Creek might not be the best representation of a high-grade ore from this deposit, although it is difficult to say since the mine is no longer operating. No amphiboles or serpentine-group minerals were detected in these samples via powder XRD.

Bulk XRF

Bulk XRF results are presented as major and minor rock-forming oxides in Table 1 (see APPENDIX A). A rock entirely composed of talc would have 63.37 weight percent SiO_2 and 31.88 weight percent MgO. In general, the results for these five samples show small deviations from pure talc. The values for Al_2O_3 in all the samples relate to the clinochlore content in the sample. Aluminum may substitute for Si in Si-deficient environments, but we know the talc-forming fluids were Si-rich so this scenario does not apply. Clinochlore, represented as $Mg_5Al(AlSi_3)O_{10}(OH)_8$, also is responsible for the higher loss on ignition (LOI) values. The LOI values indicate the weight percent of the sample that was volatized during sample preparation in the furnace; in the case of talc and clinochlore, the samples de-hydroxylated. The FeO detected represents ferric and ferrous iron combined, and is present in all samples from 1.26-2.78 weight percent. These values are not unusual in talc,

which can have minor substitutions of Fe in the octahedral site for Mg. The rest of the oxides are present in negligible concentrations and do not indicate the presence of any other phases.

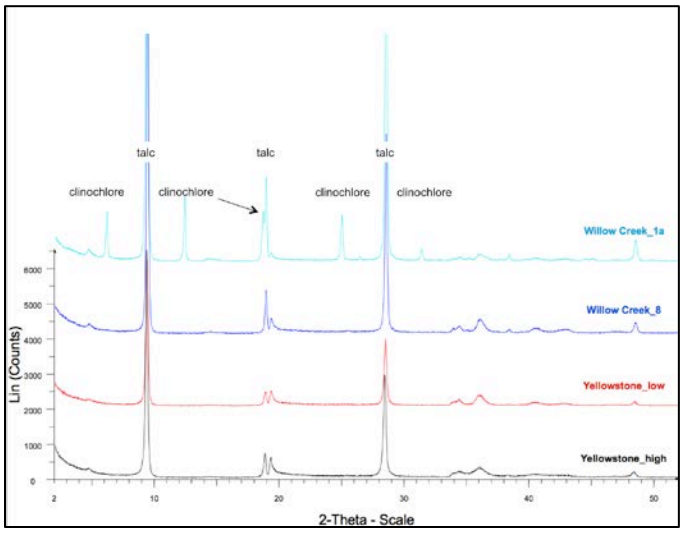

Figure 5A. Powder XRD spectra for samples from the Yellowstone and Willow Creek Mines.

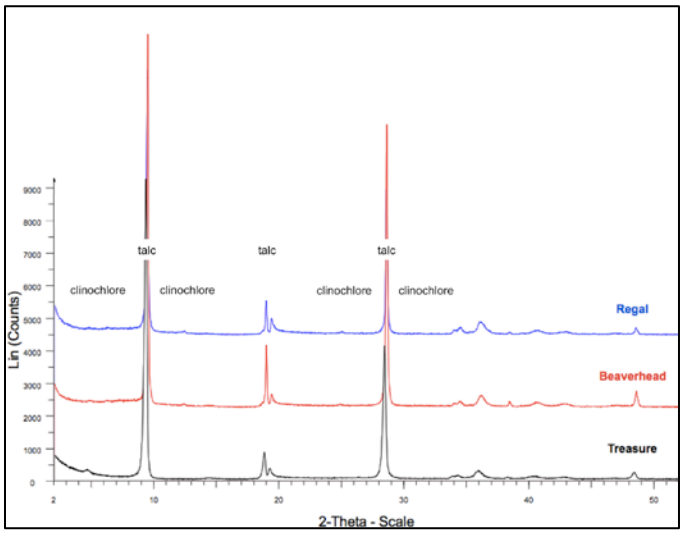

Figure 5B. Powder XRD spectra for samples from Regal, Beaverhead and Treasure Mines.

The trace element concentrations, reported in ppm, are included in Table 2 (see APPENDIX A). Trace elements are often helpful in determining provenance or understanding geologic processes. Due to the intense hydrothermal alteration of these rocks, it is likely that trace element concentrations would be more representative of the process rather than the protolith. It is worth noting that the data for the five samples are relatively uniform. This may not be surprising for samples from the same mine, but values do not vary between samples from different ranges, suggesting that the same process controlled the trace element concentrations within these deposits.

EPMA

Figures 6-13 (see Appendix B) are BSE and XPL images of the points that were analyzed by the electron microprobe. The ink circles have 2-3mm diameters, and a 100µm scale-bar is in each BSE image. In all sets of photos, the BSE images are on the top and XPL images are on the bottom. Yellow triangles indicate sampling points for talc, blue squares indicate analyses for clinochlore. The average atomic number of each phase is related to the shade of gray in the BSE images. Minerals with a higher average atomic number are lighter in the images. This is helpful in distinguishing clinochlore from talc in the sample from the Beaverhead Mine (Figure 13). Some of the images have minute differences in shades of gray, which is a result from an uneven polish on the talc due to its softness.

The compositional data from EPMA are compiled in Table 3 (see APPENDIX A). Corresponding atoms per formula unit (APFU) values are listed in Table 4 (see APPENDIX A)**.** APFU values indicate that all the talc analyzed has near end-member compositions. The low values for Al_2O_3 compared with the XRF values indicate that the Al is definitely in the clinochlore, and not substituting for Si in talc. The FeO in the talc correlates fairly well with the bulk XRF data for FeO, indicating that all the Fe is in the talc, substituting for Mg^{2+}. The clinochlore data from the Beaverhead Mine also indicate a near end-member composition. Similar to the talc, trace amounts of Fe are substituting for Mg^{2+}. We were not expecting Fe to be present in detectable quantities in this talc because of its carbonate origin. Potential sources for Fe in the talc and clinochlore may be from adjacent rocks (similar to how the gneiss provided Si, the Fe from biotite may have been released during the influx of Mg during M_2), or the initial limestone. Before M_1, the protolith may have contained some clays, which would have provided Fe and Al for the chlorite inclusions as well.

Important textural relationships to point out are the relatively fine grain sizes, irregularly shaped grains, and lack of foliation. The samples from the Beaverhead, Regal, Treasure, and Willow Creek mines (Figures 6, 7, 10-13) have a random distribution of medium to very fine- grained talc. The samples from the Yellowstone Mine (Figures 8 and 9) are both very fine-grained. These differences may be due to the textures present in the high-grade marbles that have been preserved despite the thorough talc mineralization. The samples from the Willow Creek Mine are texturally distinct in that there are halos of very fine talc that are relatively optically continuous (sections of each halo go extinct together). Although the mesh texture has been eliminated, this is most likely a talc pseudomorph after serpentinized olivine, retaining the rounded shape of the original porphyroblast. This is best seen in Figure 7, and is common throughout the rest of the thin section. However, no serpentine of olivine remnants were found in this this section; again this is evidence of complete replacement if the preexisting rock to form talc.

We conclude that commercial talc from southwest Montana is pure in that it is nearly monomineralic, the talc itself has nearly an end-member composition, and there are very low concentrations of trace elements. Although the deposits can be as far as 60 miles from each other, they share the same geologic history. The occurrences of tremolite in close proximity to the mineable bodies represent higher-grade metamorphic conditions, and do not represent the mineralogy produced by M_3.

ACKNOWLEDGEMENTS

We would like to thank Richard Berg, Imerys Talc, and Barretts Minerals for providing samples for this project; Sandra Underwood, John Childs, Chad Walby, Helen Lynn, Zachary Wall, Mike Cerino and Ericka Bartlett for organizing a very informative GSA field trip to the Regal and Yellowstone Mines; Cody Steven for help with sample preparation; and Owen Neil and Rick Conrey for their help with analyzing these samples.

DISCLOSURE

M.E. Gunter is currently working with past and current producers of talc, and has served as an expert witness for their defense; however, no funds or input from any source was directly used for the preparation of this manuscript.

REFERENCES

1. Anderson, Dale L., Mogk, David W., and John F. Childs (1990), "Petrogenesis and Timing of Talc Formation in the Ruby Range, Southwestern Montana", *Economic Geology*, vol. 85, 585-600.

2. Berg, Richard B. (1979) "Talc and chlorite deposits in Montana", *Montana Bureau of Mines and Geology*, Memoir 45.

3. Brady, J.B., Cheny, J.T., Rhodes, A.L., Vasquez, A., Green, C., Duvall, M., Kogut, A., Kaufman, L., and Dana Kovaric (1998) "Isotope geochemistry of Proterozoic talc occurrences in Archean

marbles of the Ruby Range Mountains, southwest Montana, U.S.A." *Geological Materials Research* v.1, n.2, p. 1-41.

4. Cerino, M.T., Childs, J.F., and Richard Berg (2007) "Talc in southwestern Montana", *Northwest Geology*, v.36, 9-22.
5. Chidester,A.H, Engel, A.E.J., and L.A. Wright (1964) "Talc Resources of the United States", *Geological Survey Bulletin 1167*.
6. Code of Federal Regulations, 29CFR§1910.1001(b)
7. Dahl, Peter S. (1979) "Comparative geothermometry based on major-element and oxygen isotope distributions in Precambrian Metamorphic rocks from southwestern Montana", *American Mineralogist*, vol. 64, 1280-1293.
8. Gammons, C.H. and Matt, D.O (2002) "Using fluid inclusions to help unravel the origin of hydrothermal talc deposits in southwest Montana", *Northwest Geology*, vol. 31, 44-55.
9. Giletti, B.J. (1966), "Isotopic ages from southwestern Montana", *Journal of Geophysical Research"*, vol. 71, issue 16, 4029-4036.
10. James, H.L. and Hedge, C.E. (1980), "Age of basement of southwestern Montana", *Geological Society of America Bulletin*, vol. 91, pt. 1, 1-11.
11. Johnson, D.M., Hooper, P.R., and Conrey, R.M. (1999) "Analysis of Rocks and Minerals for Major and Trace Elements on a Single Low Dilution Li-tetraborate Fused Bead", *Advances in X-ray Analysis*, vol. 41, 838-876.
12. McCarthy, E.F., Genco, N.A., and Reade E.H. Jr. (2006) "Talc", *Industrial Minerals and Rocks,* 971-986.
13. Moine, B., Fortune, J., Moreau, P., and Francis Viguier (1989) "Comparative mineralogy, geochemistry and conditions of formation of two metasomatic talc and chlorite deposits: Trimouns (Pyrenees, France) and Rabenwald (Eastern Alps, Austria), *Economic Geology*, vol. 84, 1398-1416
14. Tornos, Fernando and Baruch F. Spiro (2000) "The geology and isotope geochemistry of the talc deposits of Puebla de Lillo (Cantabrian Zone, Northern Spain)" *Economic Geology*, vol. 95, 1277-1296.
15. Underwood, S.J., Childs, J.F., Walby, C.P., Lynn, H.B., Wall, Z.S., Cerino, M.T. and Ericka Bartlett (2014) "The Yellowstone and Regal talc mines and their geologic setting in southwestern Montana", *Geologic Society of America Field Guides*, 37: 161-187.
16. Van Gosen, B.S., Lowers, H.A., Sutley, S.J., and Carol A. Gent (2004) "Using the geologic setting of talc deposits as an indicator of amphibole asbestos content", *Environmental Geology*, vol. 45, 920-939.
17. Virta, Robert L. (2015) "Talc and Pyrophyllite", *Mineral Commodity Summaries*, pp 158-159.
18. Weeks, R.L (1984), Willow Creek Mine Evaluation.
19. Zharikov, V.A., Pertsev, N.N., Rusinov, V.L., Callegari, E., and D.J. Fettes (2007), "A systematic nomenclature for metamorphic rocks 9: Metasomatism and metasomatic rocks", *Recommendation by the IUGS Subcommission on the Systematics of Metamorphic Rocks,* web version of 01.01.07.

APPENDIX A

Table 1. Bulk XRF major and minor oxide concentrations (weight percent).

Sample Name	SO3 >/=	SiO2	TiO2	Al2O3	FeO*	MnO	MgO	CaO	Na2O	K2O	P2O5	Sum	LOI (%)
Ideal	**0.00**	**63.37**	**0.00**	**0.00**	**0.00**	**0.00**	**31.88**	**0.00**	**0.00**	**0.00**	**0.00**	**95.25**	**4.75**
WC_1A	0.00	56.28	0.01	3.53	2.79	0.02	29.83	0.01	0.01	0.01	0.00	92.50	8.12
WC_8	0.00	60.73	0.00	2.73	1.34	0.01	29.88	0.01	0.03	0.01	0.00	94.73	4.82
YE_high	0.00	62.03	0.02	1.20	1.26	0.00	30.54	0.01	0.02	0.00	0.00	95.09	4.70
YE_low	0.00	62.92	0.00	0.31	1.42	0.00	30.78	0.01	0.00	0.00	0.00	95.45	4.68
TR_float	0.00	61.47	0.011	1.17	2.79	0.09	29.51	0.02	0.05	0.01	0.006	95.13	4.92

Table 2. Bulk XRF trace element concentrations (ppm) showing consistency between samples across the three ranges.

Sample Name	Ni	Cr	Sc	V	Ba	Rb	Sr	Zr	Y	Nb	Ga	Cu	Zn	Pb	La	Ce	Th	Nd	U
WC_1A	25	18	2	11	24	0	1	6	3	3.1	5	5	21	6	2	2	0	0	0
WC_8	16	22	2	4	0	0	0	0	1	1.3	4	7	13	2	1	0	0	0	2
YE_high	19	10	2	3	4	0	0	4	3	3.8	1	4	12	4	1	1	0	0	0
YE_low	9	4	1	4	1	0	0	0	1	1.1	1	1	12	3	0	0	0	0	0
Tr_float	12	10	2	5	3	0	0	2	4	2.7	2	3	15	5	0	5	0	0	0

Table 3. EPMA results, weight percent oxide.

Sample Name	SiO_2	Al_2O_3	TiO_2	ZnO	Cr_2O_3	FeO	NiO	MnO	MgO	CaO	Na_2O	K_2O	P2O5	F	Total
Ideal talc	**63.37**	**0.00**	**0.00**	**0.00**	**0.00**	**0.00**	**0.00**	**0.00**	**31.88**	**0.00**	**0.00**	**0.00**	**0.00**	**0.00**	**95.25**
WC_1a	62.24(70)	0.06(4)	0.01(1)	-	-	1.63(64)	-	0.01(1)	30.83(48)	0.02(2)	0.02(2)	0.01(2)	0.00(1)	0.19(5)	94.8(1.2)
WC_8a	62.47(56)	0.05(8)	0.00(1)	-	-	1.88(51)	-	0.01(1)	30.82(41)	0.01(1)	0.02(1)	0.01(1)	0.00(1)	0.15(2)	95.3(1.0)
YE_high	62.13(77)	0.14(1)	0.00(2)	-	-	1.09(3)	-	0.00(1)	30.93(50)	0.03(1)	0.03(1)	0.00(0)	0.01(1)	0.29(2)	94.4(1.3)
YE_low	62.66(54)	0.07(1)	0.01(1)	-	-	1.36(2)	-	bdl	31.08(32)	0.04(2)	0.00(0)	0.00(1)	0.00(1)	0.31(2)	95.20(84)
TR_float	61.87(36)	0.19(7)	0.01(1)	-	-	2.70(54)	-	0.05(4)	30.34(22)	0.03(2)	0.03(1)	0.01(1)	0.00(1)	0.20(6)	95.23(98)
RE	62.07(63)	0.21(5)	0.01(0)	0.00(1)	0.00(1)	0.52(13)	0.00(0)	0.00(1)	30.44(41)	0.02(1)	0.06(1)	0.00(0)	-	0.10(1)	93.33(72)
TR_G1	62.06(45)	0.10(4)	0.00(0)	0.01(1)	0.00(1)	0.79(95)	0.00(0)	0.00(0)	30.32(68)	0.01(0)	0.02(1)	0.00(0)	-	0.16(8)	93.32(46)
TR_G3	61.88(51)	0.16(3)	0.00(0)	0.00(1)	0.00(1)	2.24(12)	0.01(1)	0.00(0)	29.19(25)	0.02(0)	0.05(1)	0.00(1)	-	0.20(1)	93.55(45)
Treasure_xst	62.06(32)	0.17(4)	0.01(0)	0.00(1)	0.00(0)	1.93(19)	0.00(1)	0.00(1)	29.63(26)	0.01(1)	0.04(1)	0.00(0)	-	0.13(2)	93.85(24)
BH	62.18(53)	0.15(10)	0.00(0)	0.00(1)	0.00(0)	0.52(38)	0.00(1)	0.00(1)	30.36(31)	0.01(1)	0.02(1)	0.00(0)	-	0.11(2)	93.25(46)
Ideal chlorite	**35.23**	**17.59**	**0.00**	**0.00**	**0.00**	**0.00**	**0.00**	**0.00**	**34.76**	**0.00**	**0.00**	**0.00**	**0.00**	**0.00**	**87.58**
***BH**	34.3(1.4)	12.19(21)	0.01(0)	0.00(1)	0.02(0)	2.19(16)	0.00(0)	0.03(0)	33.85(50)	0.07(3)	0.02(1)	0.00(0)	-	0.10(2)	82.7(1.1)

Table 4. EPMA results, converted to APFU.

Sample Name	Si4+	Al3+	Ti4+	Zn2+	Cr3+	Fe2+	Ni2+	Mn2+	Mg2+	Ca2+	Na+	K+	P	F-	OH-	O	T
Ideal talc	**4.00**	**0.00**	**0.00**	**0.00**	**0.00**	**0.00**	**0.00**	**0.00**	**3.00**	**0.00**	**0.00**	**0.00**	**0.00**	**0.00**	**2.00**	**3.00**	**4.00**
WC_1a	3.98(0)	0.00(0)	0.00(0)	-	-	0.09(3)	-	0.00(0)	2.94(3)	0.00(0)	0.00(0)	0.00(0)	0.00(0)	0.04(1)	1.96(1)	3.03(1)	3.99(1)
WC_8a	3.98(1)	0.00(1)	0.00(0)	-	-	0.10(3)	-	0.00(0)	2.93(2)	0.00(0)	0.00(0)	0.00(0)	0.00(0)	0.03(0)	1.97(0)	3.03(2)	3.99(1)
YE_high	3.98(1)	0.01(0)	0.00(0)	-	-	0.06(0)	-	0.00(0)	2.96(1)	0.00(0)	0.00(0)	0.00(0)	0.00(0)	0.06(0)	1.94(0)	3.01(1)	3.99(0)
YE_low	3.99(0)	0.00(0)	0.00(0)	-	-	0.07(0)	-	0.00(0)	2.95(1)	0.00(0)	0.00(0)	0.00(0)	0.00(0)	0.06(0)	1.94(0)	3.02(1)	3.99(1)
TR_float	3.96(1)	0.01(0)	0.00(0)	-	-	0.14(3)	-	0.00(0)	2.90(1)	0.00(0)	0.00(0)	0.00(0)	0.00(0)	0.04(1)	1.96(1)	3.05(2)	3.98(1)
TR_G1	4.01(1)	0.01(0)	0.00(0)	0.00(0)	0.00(0)	0.04(5)	0.00(0)	0.00(0)	2.92(6)	0.00(0)	0.00(0)	0.00(0)	-	0.03(2)	1.97(2)	2.97(3)	4.01(1)
RE	4.01(2)	0.02(0)	0.00(0)	0.00(0)	0.00(0)	0.03(1)	0.00(0)	0.00(0)	2.93(3)	0.00(0)	0.01(0)	0.00(0)	-	0.02(0)	1.98(0)	2.97(3)	4.01(1)
BH	4.02(2)	0.01(1)	0.00(0)	0.00(0)	0.00(0)	0.03(2)	0.00(0)	0.00(0)	2.92(3)	0.00(0)	0.00(0)	0.00(0)	-	0.02(0)	1.98(0)	2.96(4)	4.02(2)
Ideal chlorite	**3.00**	**2.00**	**0.00**	**0.00**	**0.00**	**0.00**	**0.00**	**0.00**	**5.00**	**0.00**	**0.00**	**0.00**	**0.00**	**0.00**	**2.00**	**6.00**	**4.00**
***BH**	3.36(8)	1.41(4)	0.00(0)	0.00(0)	0.00(0)	0.18(1)	0.00(0)	0.00(0)	4.96(11)	0.01(0)	0.00(0)	0.00(0)	-	0.03(0)	7.97(0)	5.93(7)	4.00(0)

APPENDIX B

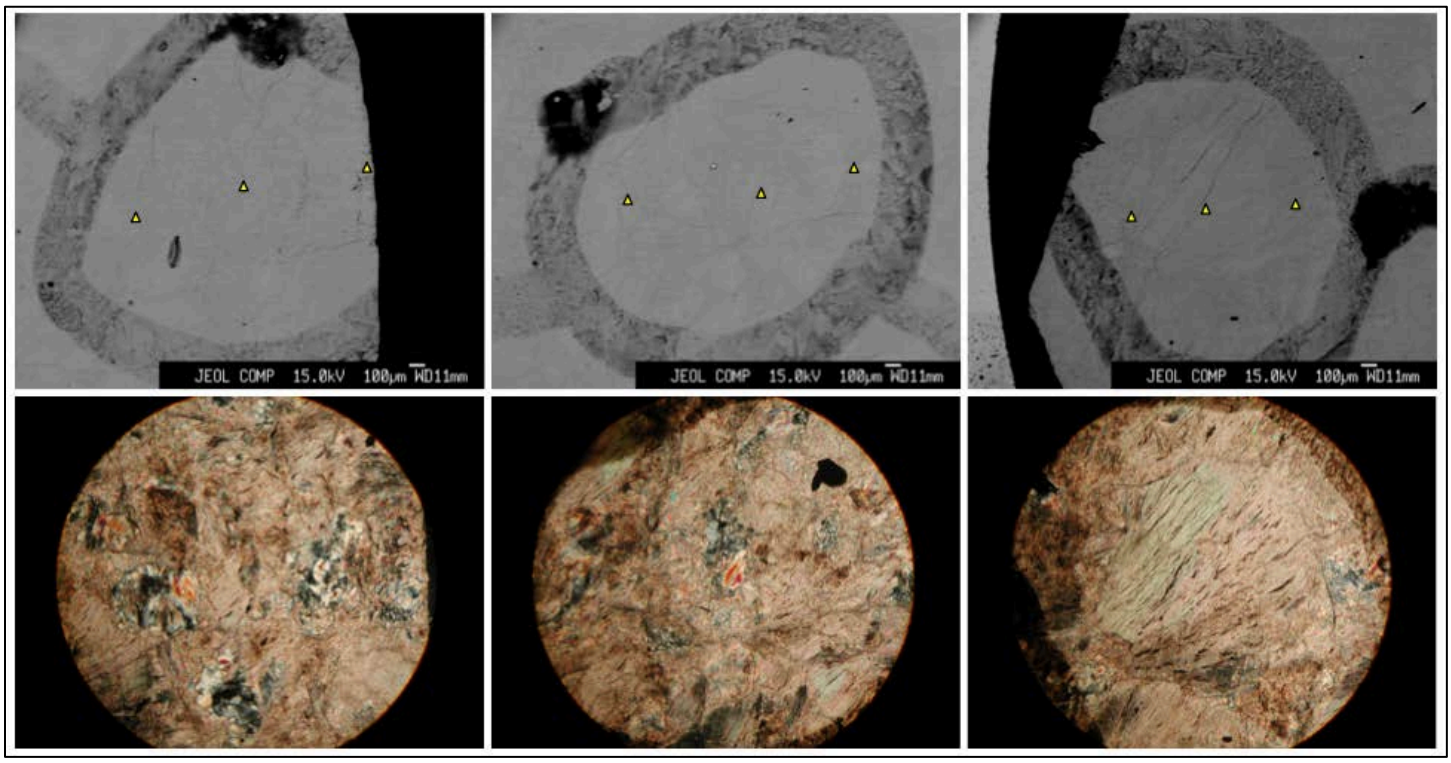

Figure 6. BSE (top) and XPL (bottom) images for WC_1a. Note the variability in grain sizes.

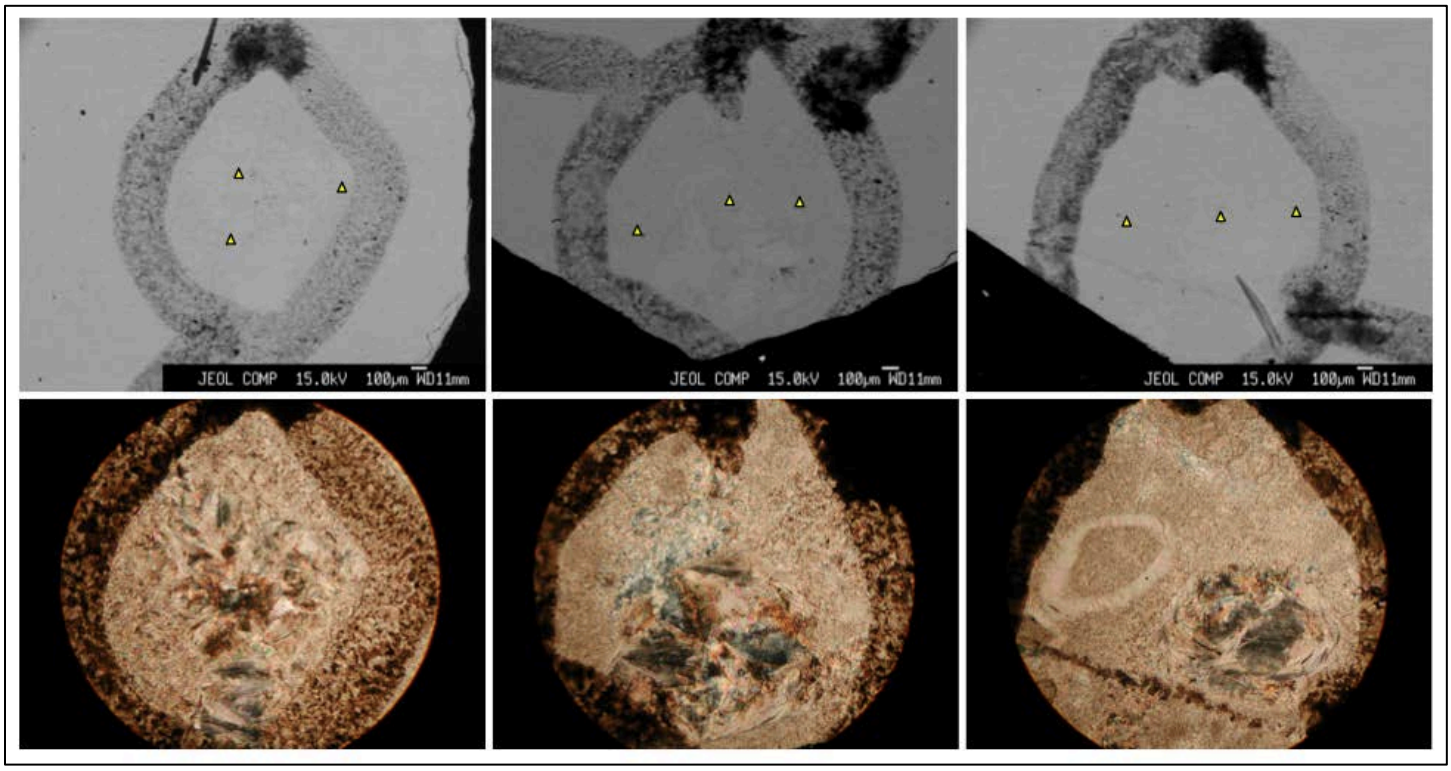

Figure 7. BSE (top) and XPL (bottom) images for WC_8a. Note the variability in grain sizes and the talc halo.

APPENDIX B (cont'd)

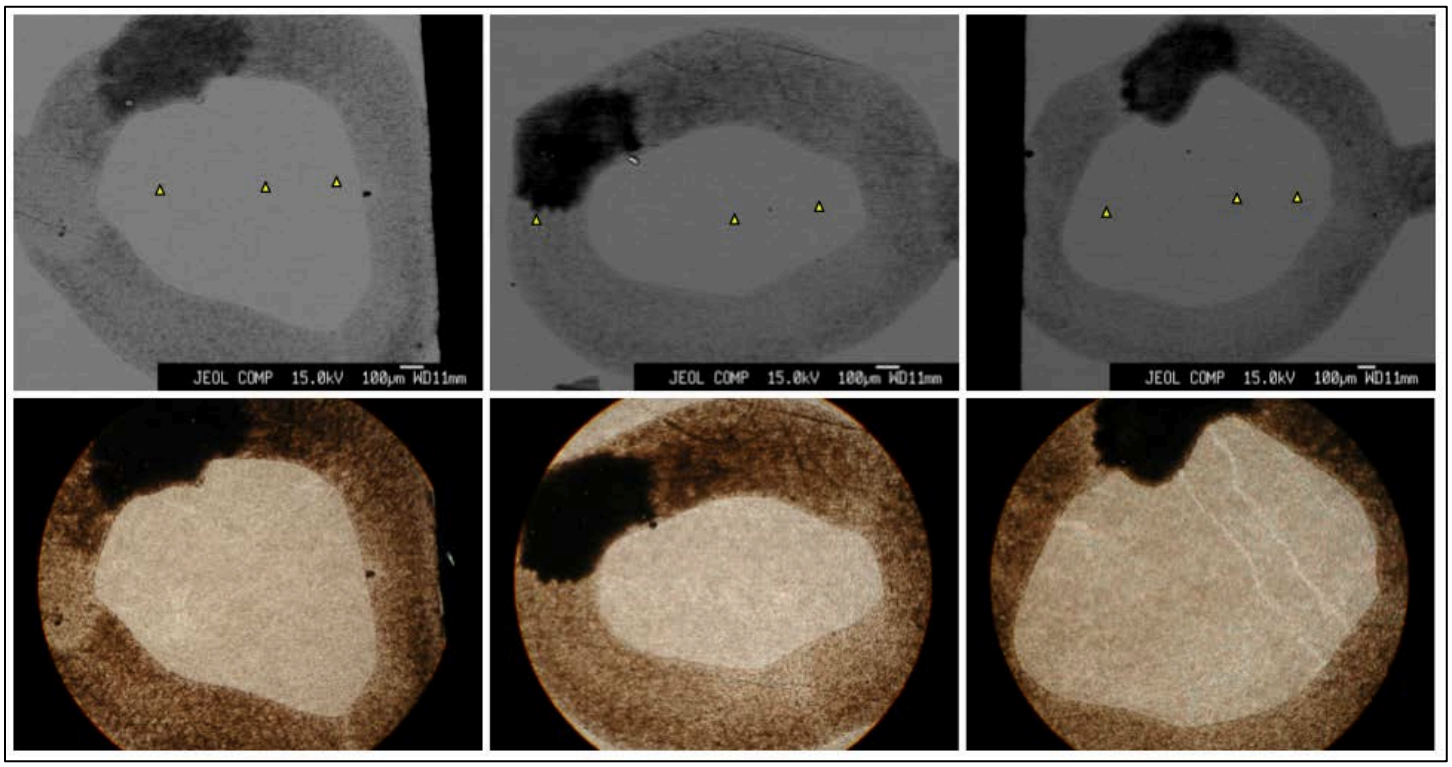

Figure 8. BSE (top) and XPL (bottom) images for YE_high. Note the very fine and uniform grain sizes.

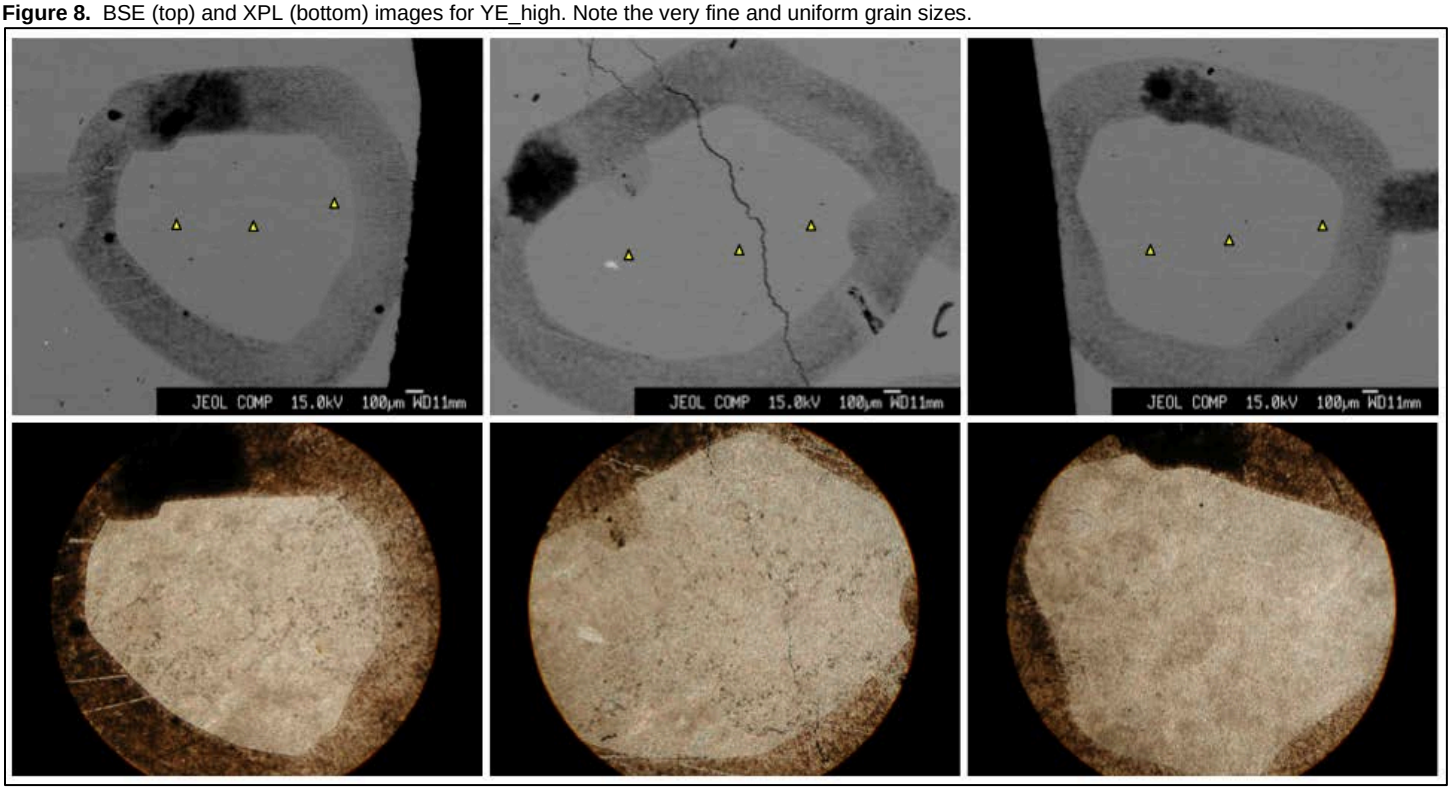

Figure 9. BSE (top) and XPL (bottom) images for YE_low. Note the very fine and uniform grain sizes.

APPENDIX B (cont'd)

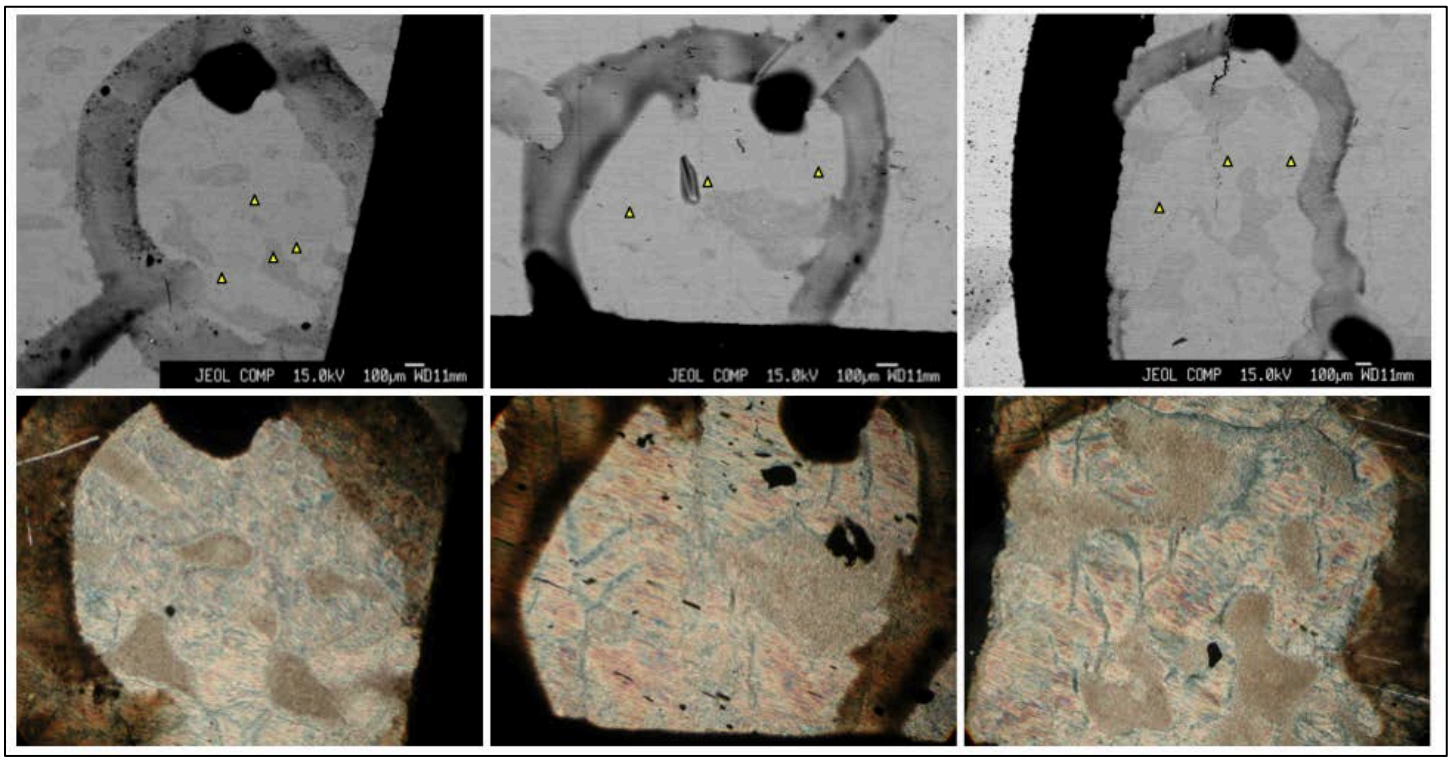

Figure 10. BSE (top) and XPL (bottom) images for TR_float

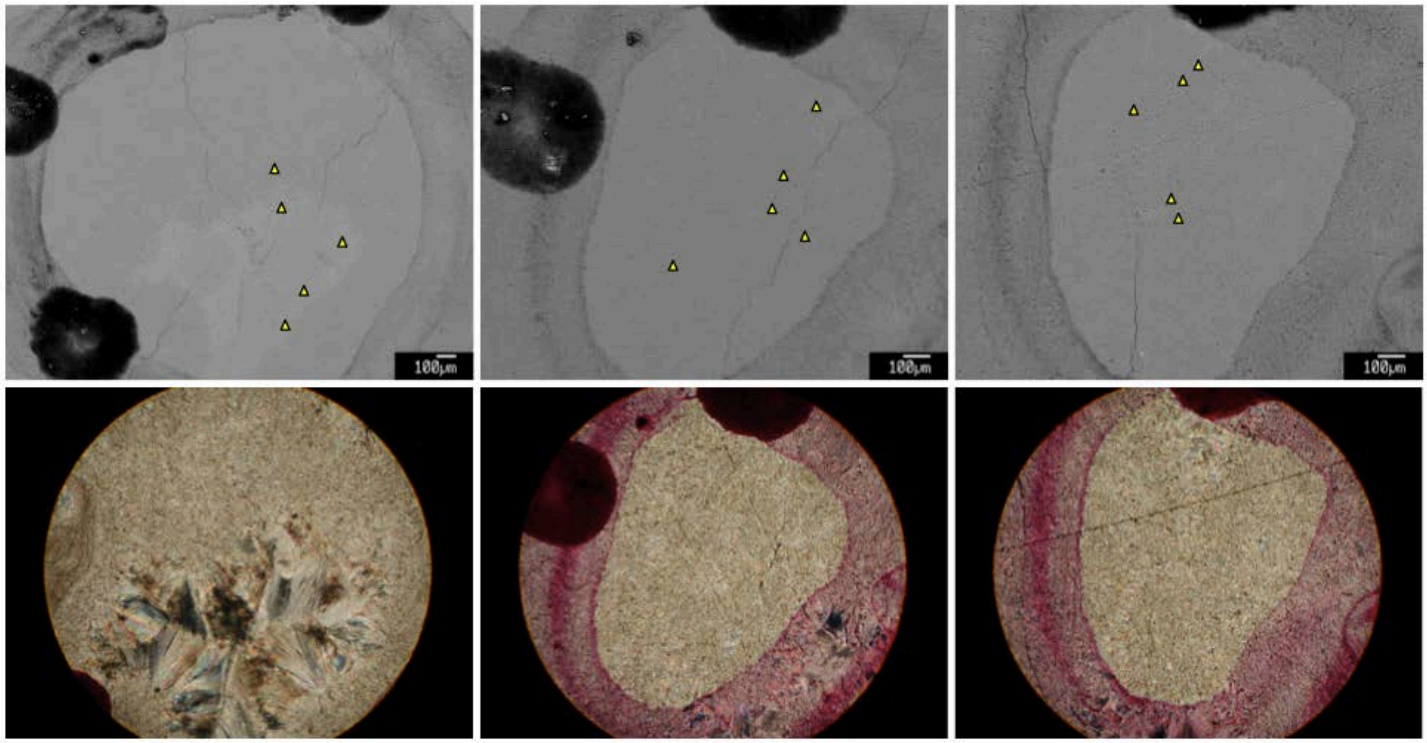

Figure 11. BSE (top) and XPL (bottom) images for TR_G1.

APPENDIX B (cont'd)

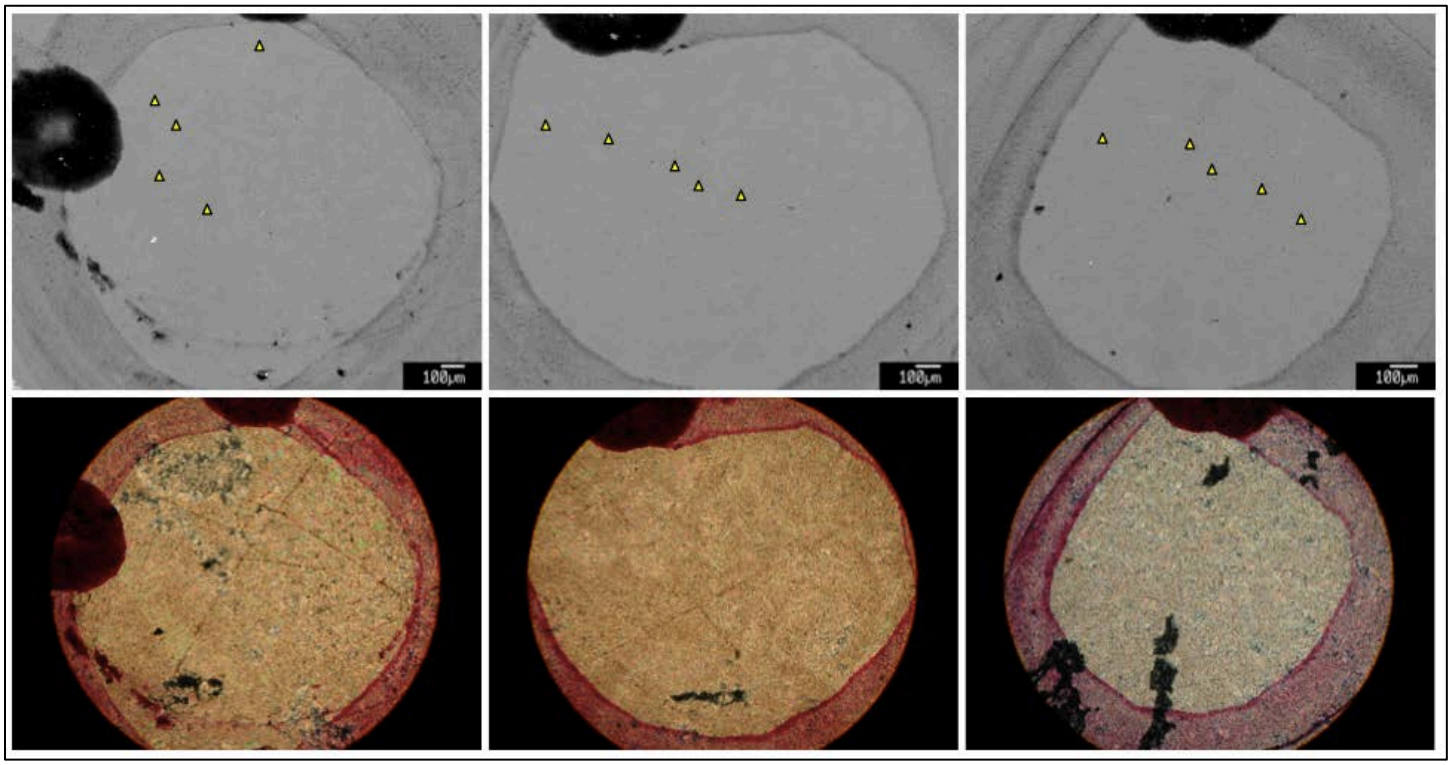

Figure 12. BSE (top) and XPL (bottom) images for RE.

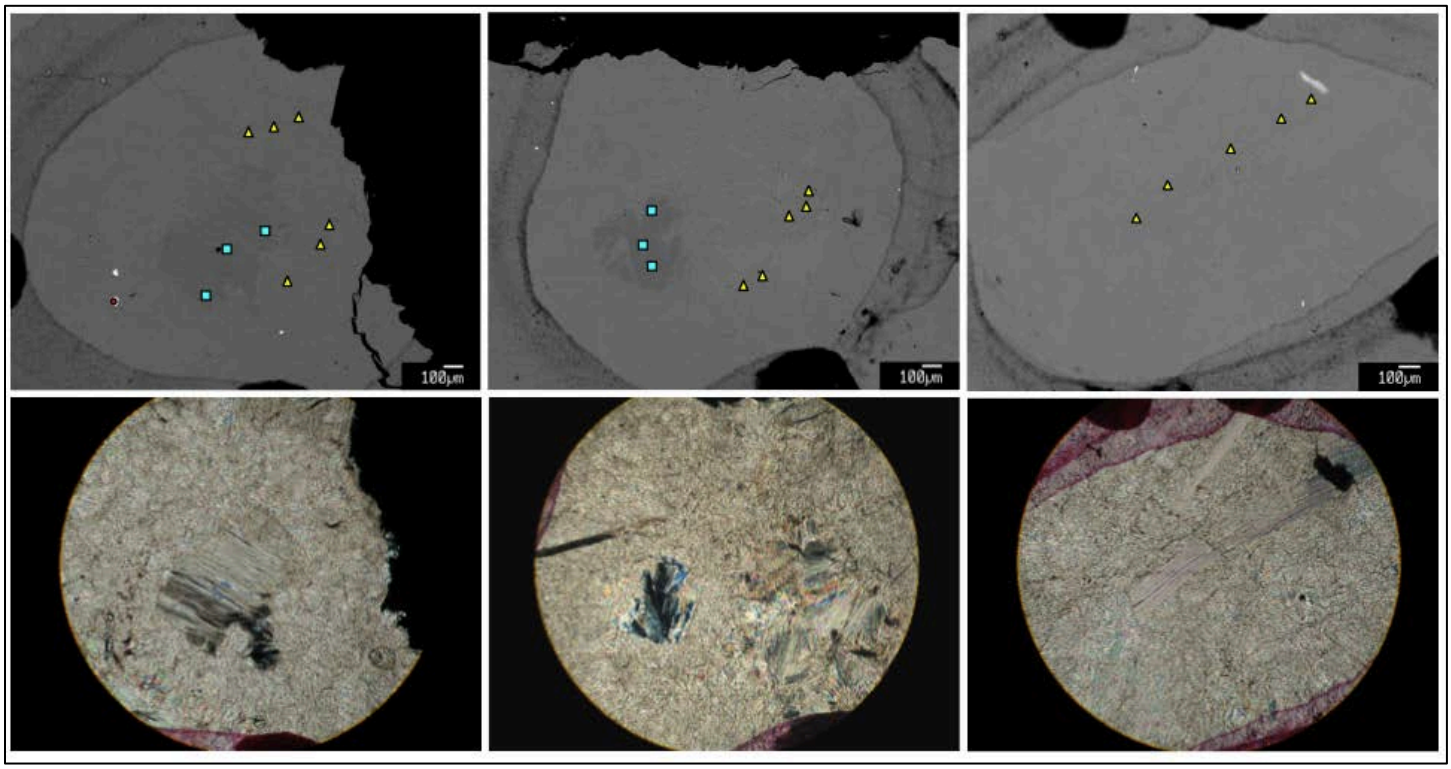

Figure 13. BSE (top) and XPL (bottom) images for BH.